Proceedings of the 41st IEEE
Conference on Decision and Control
Las Vegas, Nevada USA, December 2002

Analysis of bird formations

Pete Seiler, Aniruddha Pant, and Karl Hedrick
Email: {pseiler, pant, khedrick}@vehicle.me.berkeley.edu
Department of Mechanical Engineering
University of California at Berkeley [1]

Abstract

Birds in V formations are frequently observed and two main hypotheses have emerged in the biology/ornithology literature to explain this particular geometry: (i) it offers aerodynamic advantages and (ii) it is used to improve visual communication. Both explanations require a bird to track its predecessor. Observations of flocks suggest that this task is difficult for birds in large formations. In this paper, we explain this phenomenon using a simple bird model and systems theory. This result has implications for the coordinated control of unmanned aerial vehicles. In particular, predecessor-following is an inherently poor strategy for formation flight.

1 Introduction

Bird flocks are frequently observed in nature and numerous reasons have been proposed for this behavior. Flocking may simply be a natural social behavior [1] or it may be driven by the need to avoid, detect, and defend against predators [2]. The coordination exhibited in some bird formations suggests additional motivations. For example, traveling birds are frequently seen in linear formations such as the V, J, or echelon. Using the terminology introduced by Heppner [3], the J and echelon are variants of the V formation where one leg of the formation is shorter or is missing entirely. Two predominant hypotheses exist to explain the frequent observation of linear formations. One hypothesis is that birds gain some aerodynamic advantage when in a linear formation [4]. The alternative hypothesis is that visual communication between flock members is improved leading to enhanced navigation capabilities [5, 3]. We will give a brief review of these two hypotheses.

An aerodynamic advantage is obtained by flying in the upwash produced by other birds in the formation [4, 6, 7, 8]. Specifically, a pair of trailing vortices form 1 to 2 wingspans behind a bird [9, 6]. Based on a fixed-wing analysis, the distance between these vortices is $\frac{\pi}{4}b$

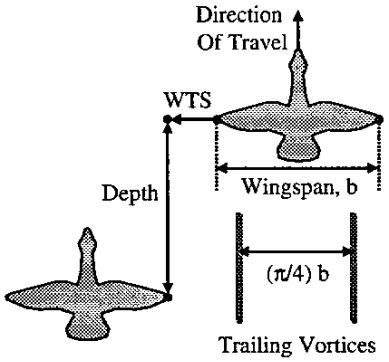

Figure 1: Formation Notation

where b is the wingspan of the bird [9, 7, 8] (see Figure 1). Within the trailing vortices is an area of downwash and outside the vortices is an area of upwash. To obtain maximum lift from this upwash, birds should fly with a wingtip spacing (WTS) of $WTS_{opt} = (\frac{\pi}{4}-1)\times\frac{b}{2}$. $WTS_{opt} < 0$ which implies that the bird wings should overlap to take full advantage of the upwash. The savings are strongly dependent on lateral position, so a trailing bird must accurately track WTS_{opt}. On the other hand, a consequence of Munk's displacement theorem is that the savings are, more or less, independent of the longitudinal position [4, 7]. Thus a bird formation can be staggered to distribute the load evenly among its members without affecting the total induced drag [4, 7]. We should note that these results are based on a fixed wing analysis. As noted in [10], the results are likely to be valid for birds with large wing spans and low wingbeat frequency, for example a Canada Goose in steady flight.

The visual communication hypothesis postulates that formation geometry is correlated with retinal features and the location of the eye on the head [5, 3, 11, 10]. For example, Heppner [3] speculated that the placement of the eyes restricts the field of vision and this motivates the use of a V formation. The enhanced visual communication may benefit bird flocks in several ways. First, it may aid migratory navigation by averaging the desired directions of all birds [5]. This ensures the flock saves time and energy by taking the most direct mi-

[1]This work was supported in part by Office of Naval Research (ONR) under the grant N00014-99-10756.

0-7803-7516-5/02/$17.00 ©2002 IEEE

gratory route [10]. The enhanced visual communication may also increase the probability that flocks are maintained during flight between roosting and foraging areas [12]. This would enable group activities to be performed at the destination. Finally, the enhanced visual communication may enable younger birds to learn about migratory paths and/or traditional roosting and feeding areas [13].

These two hypotheses lead to different predictions on the relationships between WTS and depth. The aerodynamic advantage hypothesis predicts that WTS will be close to WTS_{opt} with small variance and a positive skew ($WTS \geq WTS_{opt}$). Furthermore, the WTS should be uncorrelated with depth [10]. The visual communication hypothesis predicts that WTS and depth will be positively correlated to maintain the optimal angle between birds [10].

Many researchers have observed and studied bird formations with the goal of testing the predictions generated by these hypotheses [5, 14, 15, 12, 16, 17, 10, 18, 13]. The evidence contained in this body of literature appears to support the idea that the aerodynamic advantages may be the dominant factor for some birds, such as the Canada Goose [16, 10] and the Greylag Goose [13]. Badgerow [10] argued that biomechanical reasons make it particularly important for the Canada Goose to take advantage of the upwash of neighboring birds. On the other hand, observations of the Pink-footed Goose, a relatively smaller bird, favor the visual communication hypothesis [18].

Both hypotheses require a bird to track the lateral position of its predecessor. Two observations in this body of literature imply that this task is difficult for birds in large formations. First, the distribution of wingtip spacings within a formation commonly has a large variation (Table 1). Hainsworth [16] offers anecdotal evidence of this variation:

> My observations of flight under windy conditions suggest frequent changes in direction, propagated 'oscillations' along the length of V legs, and a more frequent break-up and reformation of Vs.

Second, the formation size appears to be relatively small on average. Table 1 gives an estimate of formation sizes observed in various references. If we assume that all these formations are Vs, then a typical leg contains only 4-5 birds. Hainsworth [16] noted a further stratification of formations into smaller sub-formations.

Similar observations appear in the control literature in the context of vehicle following. The amplification of disturbances as they propagate down a chain of vehicles, commonly known as *string instability*, has been studied by many researchers, including [19, 20, 21, 22]. String instability limits the sizes of vehicle platoons and makes it difficult to achieve tight tracking. This error damping property has been extended to multiple dimensions [23] and nonlinear systems [24]. In this paper, we derive a general string stability result and use it to explain the small formations and poor tracking observed in bird flocks. Previous results have shown that the predecessor-following strategy is string unstable for specific control laws. Our result shows that it is string unstable for *any* linear controller.

Ref.	# of Formations Observed	Range of Observed WTS (cm)	Average Formation Size (No. of Birds)
[16]	8	[-171, 183]	8
[17]	14	[-130, 289]	3
[10]	50	?	Majority < 12
[18]	54	[-90, 189]	7
[13]	25	[-100, 160]	11

Table 1: Observed Formation Data (Formation sizes are only estimates due to the actual data reported in a given reference)

The remainder of this paper has the following structure: A bird model and notation are given in the next section. In Section 3, we prove an integral inequality for the complementary sensitivity function. We apply this inequality to explain the difficulty birds have maintaining accurate spacing in large formations. In Section 4 we discuss the implications of this result for control.

2 Bird Formation Model

In this section we present a model for a V-formation of birds. The first step is to define the notation for the V formation (Section 2.1). Then we describe the dynamics of an individual bird (Section 2.2).

2.1 Formation Notation

We model each leg of the linear formation as a string of $(N+1)$ birds. Let $p_0(t) \in \mathbb{R}^3$ denote the Cartesian position of the first bird and $p_i(t) \in \mathbb{R}^3$ $(1 \leq i \leq N)$ denote the position of the i^{th} follower bird in the string. Define the tracking errors as: $e_i(t) = (p_{i-1}(t) + \delta) - p_i(t)$ $(1 \leq i \leq N)$ where δ is the desired spacing vector. For example, if a bird wants to fly two wingspans behind his predecessor at the optimum wingtip spacing, then $\delta = [-2b \ \frac{\pi b}{2} \ 0]$. We will assume that the goal of each follower bird is to force these spacing errors to zero for an aerodynamic advantage or for visual communication.

2.2 Individual Bird Model

In this section, we model birds that are attempting to fly in formation at some steady velocity, v_{ss}. Our bird model consists of the Newtonian equations of motion and a linear model of the force generation process. In the process of estimating the power required for flight, Pennycuick [25] stated the main forces acting on a bird:

- Parasitic drag: This is the force exerted by the air on the body of a bird, excluding the wings. This force is given by $-C_D \|v\| v$ where C_D is the drag coefficient and v is the velocity vector of the bird.
- Weight: This force is given by $-mg\bar{k}$ where where m is the mass of the bird, g is the gravitational constant and $\bar{k}$ is the unit vector in the z-direction.
- Profile drag: This is the drag exerted by air on the wings when they are flapped. As a first approximation, the force is inversely proportional to the speed: $-\frac{C_P}{\|v\|^2} v$ where C_P is the profile drag coefficient.
- Lift and Thrust: The bird is able to generate lift and thrust by flapping its wings. We denote the sum of these forces by F.

Let $p = [x\ y\ z]^T$ be the Cartesian position of the bird. Newton's law gives the equations of motion for the bird:

$$m\ddot{p} = -C_D \|v\| v - mg\bar{k} - \frac{C_P}{\|v\|^2} v + F \qquad (1)$$

We note that to maintain a steady velocity, $v = v_{ss}$, the lift and thrust must balance all other forces on the bird: $F_{ss} = C_D \|v_{ss}\| v_{ss} + mg\bar{k} + \frac{C_P}{\|v_{ss}\|^2} v_{ss}$

Next we model the force generation process. In a formation, the bird is attempting to track the position of the preceding bird, modulo some offset. To accomplish this task, the bird must sense the tracking error, e, and take some corrective action. We assume the sensory dynamics of the eyes, the tracking algorithm in the brain, and the flight mechanics of the force generation can be approximately modeled as a finite dimensional nonlinear dynamical system:

$$\dot{z} = h_1(z, e)$$
$$F = h_2(z, e)$$

where $z \in \mathbb{R}^n$ is the state of the system and $e \in \mathbb{R}^3$ is the tracking error. These dynamics from the tracking error to the actual force generated on the bird are probably quite complex and the state dimension, n, is possibly very large. We assume that if there is no tracking error, the bird generates the necessary force to maintain the steady velocity: $h_1(0,0) = 0$ and $h_2(0,0) = F_{ss}$.

We can now linearize these complex, nonlinear dynamics:

$$\Delta\dot{z} = \overbrace{\left(\frac{\partial h_1}{\partial z}\right)_{(0,0)}}^{A} \Delta z + \overbrace{\left(\frac{\partial h_1}{\partial e}\right)_{(0,0)}}^{B} e$$
$$F = F_{ss} + \underbrace{\left(\frac{\partial h_2}{\partial z}\right)_{(0,0)}}_{C} \Delta z + \underbrace{\left(\frac{\partial h_2}{\partial e}\right)_{(0,0)}}_{D} e$$

Thus the overall system dynamics linearized about the steady state velocity are given by:

$$\ddot{p} = \frac{1}{m}\Delta F \qquad (2)$$

$$\begin{aligned} \Delta\dot{z} &= A\Delta z + Be \\ \Delta F &= C\Delta z + De \end{aligned} \qquad (3)$$

3 Formation Analysis

In this section we derive a relation for the the spacing errors in the formation (Section 3.1). We then give a technical result from systems theory (Section 3.2). We apply this result to analyze the spacing errors along one leg of a V formation (Section 3.3). The conclusion is that tight spacing control is difficult if the predecessor following strategy is employed. We will denote the spectral radius of a matrix A by $\rho[A]$ and the maximum singular value by $\bar{\sigma}(A)$.

3.1 Formation Spacing Errors

In the Laplace domain, the individual bird model (Equations 2 and 3) is given by ($1 \le i \le N$):

$$P_i(s) = \frac{1}{s^2}\underbrace{\frac{1}{m}\left[C(sI - A)^{-1}B + D\right]}_{H(s)} E_i(s) + \frac{p_i(0)}{s} + \frac{v_{ss}}{s^2} \qquad (4)$$

$p_i(0)$ is the initial position of the i^{th} bird and we assume each bird initially has the steady state velocity, v_{ss}. We assume that the formation starts with zero initial spacing error: $p_i(0) = i\delta$ for all i.

Simple algebra using the bird models (Equation 4), initial conditions, and error definitions gives the following relations:

$$E_i(s) = S(s)P_0(s) \qquad (5)$$
$$E_i(s) = T(s)E_{i-1}(s) \quad \text{for } i = 2, \ldots, N \qquad (6)$$

where

$$S(s) := \left[I + \frac{1}{s^2}H(s)\right]^{-1}$$
$$T(s) := \left[I + \frac{1}{s^2}H(s)\right]^{-1}\left[\frac{1}{s^2}H(s)\right]$$

Equation 5 shows that the transfer function matrix from $P_0(s)$ to $E_1(s)$ is the sensitivity function, $S(s)$. Equation 6 shows that the complementary sensitivity function governs the propagation of errors along the arm of the V. Thus $S(s)$ governs the first spacing error generated by the leader motion, $P_0(s)$, and $T(s)$ governs the propagation of errors away from the leader.

Let a_i denote the acceleration of the i^{th} bird. The acceleration is an indication of the effort required by the bird to maintain his position in the formation. We can obtain similar relations for the propagation of this control effort.

$$A_i(s) = T(s)A_{i-1}(s) \text{for } i = 1, \ldots, N \tag{7}$$

where $A_0(s)$ is the acceleration of the leader.

There is a classical control trade-off between making $\bar{\sigma}(S(j\omega))$ and $\bar{\sigma}(T(j\omega))$ small. Since $S(s) + T(s) \equiv I$, we cannot make $\bar{\sigma}(S(j\omega))$ and $\bar{\sigma}(T(j\omega))$ simultaneously small. Fortunately in the classical systems analysis the competing objectives occur in different frequency regions. It is typically sufficient for $\bar{\sigma}(S(j\omega))$ to be small at low frequencies and $\bar{\sigma}(T(j\omega))$ to be small at high frequencies. In the context of Equations 5-6, the $S(s)$ vs. $T(s)$ trade-off has the interpretation of limiting initial spacing error (making $\bar{\sigma}(S(j\omega))$ small) and limiting the propagation of errors (making $\bar{\sigma}(T(j\omega))$ small). In this case we cannot spread these competing objectives into different frequency bands. In other words, we would like $\bar{\sigma}(T(j\omega)) < 1$ at all frequencies so that propagating errors are attenuated.

To attenuate propagating errors in the formation, we require $\bar{\sigma}(T(j\omega)) < 1$ at all frequencies. Another measure of error amplification is given by $\rho[T(j\omega)]$. The condition $\rho[T(j\omega)] < 1$ ensures the eventual decay of all errors in the formation. This interpretation follows because the error propagation (Equation 6) is simply a discrete system at each fixed frequency. We refer to [26] for the details.

3.2 Main Result

Unfortunately $T(0) = I$ and thus neither $\bar{\sigma}(T(j\omega)) < 1$ nor $\rho[T(j\omega)] < 1$ holds for all frequencies. The interpretation is that DC errors are propagated without attenuation. Moreover, the next theorem implies that there is a frequency and a direction such that error amplification occurs. This theorem is a generalization of a SISO result by Middleton and Goodwin [27, 28]. It is similar to results obtained by Chen [29, 30].

Theorem 1 *Let $H(s)$ be an $n_p \times n_p$ rational, proper transfer function matrix and $L(s) = \frac{1}{s^2}H(s)$ be the open loop transfer function. If the closed loop system is stable, then the complementary sensitivity function, $T(s) = [I + L(s)]^{-1}L(s)$, must satisfy:*

$$\int_0^\infty \log \rho[T(j\omega)] \frac{d\omega}{\omega^2} \geq 0 \tag{8}$$

where log *is the natural* log.

Proof. This proof is similar to the proof of Theorem 4.1 in [30]. By assumption, $T(s)$ is an $n_p \times n_p$ matrix with entries that are analytic and bounded in the open right half plane. Boyd and Desoer [31] showed that $\log \rho[T(s)]$ is subharmonic and satisfies the Poisson Inequality for $x > 0$:

$$\log \rho[T(x)] \leq \frac{1}{\pi} \int_{-\infty}^{\infty} \log \rho[T(j\omega)] \frac{x d\omega}{x^2 + \omega^2} \tag{9}$$

Multiplying Equation 9 by $1/x$ and taking the limit of both sides as $x \to 0$ gives inequality (a) below:

$$\begin{aligned} \lim_{x \to 0} \frac{\log \rho[T(x)]}{x} &\overset{(a)}{\leq} \lim_{x \to 0} \frac{1}{\pi} \int_{-\infty}^{\infty} \log \rho[T(j\omega)] \frac{d\omega}{x^2 + \omega^2} \\ &\overset{(b)}{=} \frac{1}{\pi} \int_{-\infty}^{\infty} \log \rho[T(j\omega)] \frac{d\omega}{\omega^2} \\ &\overset{(c)}{=} \frac{2}{\pi} \int_{0}^{\infty} \log \rho[T(j\omega)] \frac{d\omega}{\omega^2} \end{aligned} \tag{10}$$

Equality (b) follows by applying the monotone convergence theorem [32] to the positive and negative parts of the integrand. Equality (c) follows from a conjugate symmetry property of $T(s)$: $\rho[T(-j\omega)] = \rho[T(j\omega)]$.

The proof is concluded by showing $\lim_{x \to 0}(1/x) \log \rho[T(x)] = 0$ and applying the end-to-end inequality in Equation 10. Since the open loop transfer function, $L(s)$, has two poles at $s = 0$, $T(x)$ can be expanded for sufficiently small x as:

$$T(x) = I + o(x) \text{ where } \lim_{x \to 0} \frac{o(x)}{x} = 0 \tag{11}$$

Thus $\rho[T(x)] = 1 + o(x)$ and $\log \rho[T(x)] = o(x)$ (where each $o(x)$ is, in general, a different function with the same limiting property as in Equation 11). We conclude that $\lim_{x \to 0}(1/x) \log \rho[T(x)] = 0$ as desired. ■

We apply this theorem by considering the following sets of frequencies:

$$\begin{aligned} I_1 &= \{\omega \ : \ \rho[T(j\omega)] > 1\} \\ I_2 &= \{\omega \ : \ \rho[T(j\omega)] = 1\} \\ I_3 &= \{\omega \ : \ \rho[T(j\omega)] < 1\} \end{aligned}$$

Since $\log \rho[T(j\omega)] = 0$ if $\omega \in I_2$, Equation 8 can be written as:

$$\int_{I_1} \log \rho[T(j\omega)] \frac{d\omega}{\omega^2} \geq -\int_{I_3} \log \rho[T(j\omega)] \frac{d\omega}{\omega^2} \tag{12}$$

We note that $\log \rho[T(j\omega)] < 0$ if $\omega \in I_3$. Moreover, $\rho[T(j\omega)] \to 0$ as $\omega \to \infty$ and thus I_3 is not an empty set. Consequently, the right side of Equation 12 is strictly positive and hence I_1 is a non-empty set. Continuity implies that there is an interval of frequencies where $\rho[T(j\omega)] > 1$. Moreover, $\bar{\sigma}(T(j\omega)) > 1$ at these frequencies because the maximum singular value upper bounds the spectral radius. Thus, error amplification may occur at these frequencies and along particular spatial directions. In practice, low frequency content of the error signal is amplified as it propagates.

3.3 Analysis of Spacing Errors

In this section, we summarize the result. The spacing errors are related by:

$$E_i(s) = T(s)E_{i-1}(s) \quad \text{for } i = 2, \ldots, N$$

Thus for $i > 1$, $E_i(s) = T^{i-1}(s)E_1(s)$. Furthermore, by the result in the previous section, there is an interval of frequencies such that $\rho[T(j\omega)] > 1$. If the lead bird performs a nontrivial maneuver, then we can assume, without loss of generality, that $E_1(j\omega) \neq 0$ in the given frequency interval. Consequently, $|E_i(j\omega)| \to \infty$ as $i \to \infty$ at these frequencies. In words, it is progressively more difficult for birds which are far from the leader to track the lateral position of the predecessor. Similarly, it is possible to show from Equation 7 that larger accelerations are required for birds that are far from the leader. This result is independent of the (A, B, C, D) chosen to represent the force generation dynamics (Equation 3) and relies only on the presence of the rigid body dynamics (Equation 2).

4 Implications for control

This result has similar consequences for automated formation flight. Consider a simple control strategy where each vehicle in a V formation tries to follow its predecessor. Figure 2 loop depicts a feedback loop implementing the predecessor following strategy. The reference trajectory for the i^{th} vehicle is the position of the preceding vehicle plus some desired offset, $p_{i-1} + \delta$. $H(s)$ represents any actuator dynamics required to generate a vehicle acceleration. If these dynamics are nonlinear, then linearization about an operating point or feedback linearization can be used to obtain linear actuator dynamics. $K_p(s)$ is any linear, time-invariant control law. The loop transfer function is $L(s) = \frac{1}{s^2}H(s)K_p(s)$. As in the previous section, the errors propagate via $T(s) = [I + L(s)]^{-1}L(s)$. Theorem 1 can be applied to conclude that the predecessor-following strategy is string unstable for any linear control law.

A solution to this problem is to communicate leader information to all vehicles in the formation. A linear

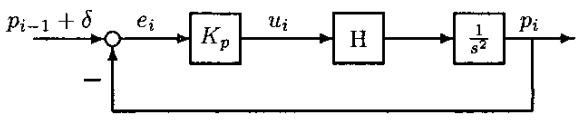

Figure 2: Predecessor Following Feedback Loop

control law using information from the lead and preceding vehicles is given by:

$$U_i(s) = K_p(s)E_i(s) + K_l(s)\left(P_0(s) - P_i(s) - \frac{(i-1)\delta}{s}\right) \tag{13}$$

This controller tries to keep the errors with respect to the preceding vehicles and with respect to the lead vehicle small. Intuitively, this control law gives each vehicle some preview information. In this case, the errors propagate as follows:

$$E_i(s) = T_{lp}(s)E_{i-1}(s) \qquad \text{for } i > 2 \tag{14}$$

where $T_{lp}(s) := [I + H(s)(K_p(s) + K_l(s))]^{-1} H(s)K_p(s)$. Now we can easily design $K_l(s)$ and $K_p(s)$ so that $\bar{\sigma}(T(j\omega)) < 1$ for all ω. This ensures that propagating errors are damped out in the formation. More details, with specific application to unmanned aerial vehicles, are given in [33].

5 Conclusions

In this paper, we reviewed two main hypotheses from ornithology that try to explain the reason for birds to fly in formation. A systems theory approach was used to show that the birds need to keep the formations small. If the formations become large, then the birds at the end of formations will have difficulty keeping their positions in the formation. The implications of the result to control of unmanned aerial vehicles were discussed in brief. It was shown that flying in close formation is not possible with information only about the predecessors. However, using communication to transmit leader state information to all the vehicles in the formation solves the problem.

References

[1] J.T. Emlen, "Flocking behavior in birds," *Auk*, vol. 69, pp. 160–170, 1952.

[2] I. Vine, "Risk of visual detection and pursuit by a predator and the selective advantage of flocking behaviour," *J. of Theoretical Biology*, vol. 30, pp. 405–422, 1971.

[3] F.H. Heppner, "Avian flight formation," *Bird Banding*, vol. 45, no. 2, pp. 160–169, 1974.

[4] P.B.S. Lissaman and C.A. Shollenberger, "Formation flight of birds," *Science*, vol. 1968, pp. 1003–1005, May 1970.

[5] L.L. Gould and F. Heppner, "The Vee formation of canada geese," *Auk*, vol. 91, pp. 494–506, July 1974.

[6] J.P. Badgerow and F.R. Hainsworth, "Energy savings through formation flight? A re-examination of the Vee formation," *J. of Theoretical Biology*, vol. 93, pp. 41–52, 1981.

[7] D. Hummel, "Aerodynamic aspects of formation flight in birds," *J. of Theoretical Biology*, vol. 104, pp. 321–347, 1983.

[8] D. Hummel, "Formation flight as an energy-saving mechanism," *Israel J. of Zoology*, vol. 41, pp. 261–278, 1995.

[9] J.J.L. Higdon and S. Corrsin, "Induced drag of a bird flock," *The American Naturalist*, vol. 112, no. 986, pp. 727–744, July-August 1978.

[10] J.P. Badgerow, "An analysis of function in the formation flight of canada geese," *Auk*, vol. 93, pp. 41–52, 1988.

[11] F.H. Heppner, J.L. Convissar, D.E. Moonan, Jr., and J.G.T. Anderson, "Visual angle and formation flight in canada geese {*Branta Canadensis*} ," *Auk*, vol. 102, pp. 195–198, January 1985.

[12] J. Brian E. O'Malley and Roger M. Evans, "Structure and behavior of white pelican formation flocks," *Canadian J. of Zoology*, vol. 60, pp. 1388–1396, 1982.

[13] J.R. Speakman and D. Banks, "The function of flight formations in Grelag Geese *Anser anser*; energy savings or orientation?," *Ibis*, vol. 140, pp. 280–287, 1998.

[14] T.C. Williams, T.J. Klonowski, and P. Berkeley, "Angle of canada goose V flight formation measured by radar," *Auk*, vol. 93, pp. 554–559, July 1976.

[15] P.F. Major and L.M. Dill, "The three-dimensional structure of airborne bird flocks," *Behavioral Ecology and Sociobiology*, vol. 4, pp. 111–122, 1978.

[16] F.R. Hainsworth, "Precision and dynamics of positioning by canada geese flying in formation," *J. of Experimental Biology*, vol. 128, pp. 445–462, 1987.

[17] F.R. Hainsworth, "Induced drag savings from ground effect and formation flight in brown pelicans," *J. of Experimental Biology*, vol. 135, pp. 431–444, 1988.

[18] C.J. Cutts and J.R. Speakman, "Energy savings in formation flight of pink-footed geese," *J. of Experimental Biology*, vol. 189, pp. 251–261, 1994.

[19] K. Chu, "Decentralized control of high speed vehicular strings," *Transportation Science*, pp. 361–384, 1974.

[20] J.K. Hedrick and D. Swaroop, "Dynamic coupling in vehicles under automatic control," in *13th IAVSD Symposium*, August 1993, pp. 209–220.

[21] D. Swaroop, *String Stability of Interconnected Systems: An Application to Platooning in Automated Highway Systems*, Ph.D. thesis, University of California at Berkeley, 1994.

[22] D. Swaroop and J.K. Hedrick, "String stability of interconnected systems," *IEEE Transactions on Automatic Control*, vol. 41, no. 4, pp. 349–356, March 1996.

[23] Pete Seiler, Aniruddha Pant, and J.K. Hedrick, "Preliminary investigation of mesh stability for linear systems," in *Proceedings of the ASME: DSC Division*, 1999, vol. 67, pp. 359–364.

[24] A. Pant, P. Seiler, and K. Hedrick, "Mesh stability of look-ahead interconnected systems," *IEEE Transactions in Automatic Control*, vol. 47, no. 2, pp. 403–407, February 2002.

[25] C.J. Pennycuick, *Bird Flight Performance: A Practical Calculation Manual*, Oxford Science Publications, 1989.

[26] P. Seiler, *Coordinated Control of Unmanned Aerial Vehicles*, Ph.D. thesis, University of California, Berkeley, 2001.

[27] R.H. Middleton and G.C. Goodwin, *Digital Control and Estimation: A Unified Approach*, Prentice Hall, Englewood Cliffs, N.J., 1990.

[28] D.P. Looze and J.S. Freudenberg, "Tradeoffs and limitations in feedback systems," in *The Control Handbook*, W.S. Levine, Ed., chapter 31, pp. 537–549. CRC Press, 1996.

[29] J. Chen, "On logarithmic complementary sensitivity integrals for MIMO systems," in *Proceedings of the American Control Conference*, June 1998, pp. 3529–3530.

[30] J. Chen, "Logarithmic integrals, interpolation bounds, and performance limitations in MIMO feedback systems," *IEEE Transactions on Automatic Control*, vol. 45, no. 6, pp. 1098–1115, June 2000.

[31] S. Boyd and C.A. Desoer, "Subharmonic functions and performance bounds on linear time-invariant feedback systems," *IMA J. of Mathematical Control and Information*, vol. 2, pp. 153–170, 1985.

[32] H.L. Royden, *Real Analysis*, Macmillan Publishing Company, 1988.

[33] P. Seiler, *Coordinated Control of Unmanned Aerial Vehicles*, Ph.D. thesis, U. of California, Berkeley, 2001.